J Ind Microbiol Biotechnol (2014) 41:913–930
DOI 10.1007/s10295-014-1439-y

BIOCATALYSIS

SIMB
Society for Industrial Microbiology and Biotechnology

Study of metabolic network of *Cupriavidus necator* DSM 545 growing on glycerol by applying elementary flux modes and yield space analysis

Markan Lopar · Ivna Vrana Špoljarić · Nikolina Cepanec · Martin Koller · Gerhart Braunegg · Predrag Horvat

Received: 18 December 2013 / Accepted: 13 March 2014 / Published online: 9 April 2014

Abstract A metabolic network consisting of 48 reactions was established to describe intracellular processes during growth and poly-3-hydroxybutyrate (PHB) production for *Cupriavidus necator* DSM 545. Glycerol acted as the sole carbon source during exponential, steady-state cultivation conditions. Elementary flux modes were obtained by the program Metatool and analyzed by using yield space analysis. Four sets of elementary modes were obtained, depending on whether the pair NAD/NADH or FAD/$FADH_2$ contributes to the reaction of glycerol-3-phosphate dehydrogenase (GLY-3-P DH), and whether 6-phosphogluconate dehydrogenase (6-PG DH) is present or not. Established metabolic network and the related system of equations provide multiple solutions for the simultaneous synthesis of PHB and biomass; this number of solutions can be further increased if NAD/NADH or FAD/$FADH_2$ were assumed to contribute in the reaction of GLY-3-P DH. As a major outcome, it was demonstrated that experimentally determined yields for biomass and PHB with respect to glycerol fit well to the values obtained in silico when the Entner–Doudoroff pathway (ED) dominates over the glycolytic pathway; this is also the case if the Embden–Meyerhof–Parnas pathway dominates over the ED.

Keywords *Cupriavidus necator* · Elementary flux modes · Glycerol · PHB · Yield space analysis

Introduction

Polyhydroxyalkanoates (PHAs) serve as carbon- and energy-storage compounds in microorganisms and genetically modified plants [5]. They are natural, biodegradable macromolecules with material traits similar to those of synthetic petrochemically derived plastics and are accessible by the biotechnological conversion of renewable sources [17]. The downside of such processes for industrial biopolymer manufacturing is still the product price. The use of different inexpensive waste materials for PHA biosynthesis is a promising strategy for reducing production costs and, at the same time, handling industrial waste-disposal problems [16]. Among all described PHAs, the homopolyester poly-3-hydroxybutyrate (PHB) is the most common representative in nature and, since decades, the most profoundly investigated.

Biodiesel is a biofuel produced through transesterification of vegetable oils or animal fats [15]. Glycerol emerging from biodiesel production (principal by-product of the process; mass ratio of biodiesel to glycerol is 9:1) at increasing quantities [14, 15], constitutes a potential carbon substrate for PHA production.

Electronic supplementary material The online version of this article (doi:10.1007/s10295-014-1439-y) contains supplementary material, which is available to authorized users.

M. Lopar · I. V. Špoljarić · N. Cepanec · P. Horvat
Department of Biochemical Engineering, Faculty of Food Technology and Biotechnology, University of Zagreb, Pierottijeva 6/IV, 10000 Zagreb, Croatia

M. Koller
Institute of Biotechnology and Biochemical Engineering, Graz University of Technology, Petersgasse 12, 8010, Graz, Austria

M. Koller · G. Braunegg
ARENA, Arbeitsgemeinschaft für Ressourcenschonende and Nachhaltige Technologien, Graz University of Technology, Inffeldgasse 23, 8010 Graz, Austria

M. Koller (✉)
Institute of Chemistry, University of Graz, Stremayrgasse 16/IV, 8010 Graz, Austria
e-mail: martin.koller@uni-graz.at

More than 300 microbial species equipped with the genetic pre-requisites to synthesize PHAs have been isolated in the past. Some of them can produce PHAs from glycerol as carbon source: *Cupriavidus necator* (formerly *Ralstonia eutropha* or *Wautersia eutropha*), *Zobellella denitrificans*, *Pseudomonas oleovorans*, *Pseudomonas corrugate*, *Burkholderia cepacia*, *Methylobacterium rhodesianum*, *Haloferax mediterranei*, *Halomonas hydrothermalis*, and *Halomonas* sp. KM-1. Among them, *C. necator* is a promising strain for industrial production of PHAs. Unfortunately, the productivities and yields of PHAs are significantly lower on glycerol than on glucose [34]. In addition, when glycerol is used as carbon source for PHAs production, unwanted fluctuation of the PHA's polydispersity as well as the reduction of molecular mass of the polymers were observed [16]. Furthermore, the specific growth rate of *C. necator* is lower on glycerol than on glucose, as growth on glycerol usually occurs very slowly [14, 48]. One possible strategy to overcome this problem is cultivation of biomass on glucose as carbon source (rapid growth) and subsequently switching to glycerol under nitrogen limitation (non-growth associated PHA synthesis). Another possibility is to keep the glucose/glycerol ratio at a suitable constant value during the phase of non-growth-associated PHA synthesis; the latter strategy is hardly feasible. Wild-type strain *R. eutropha* H16 is able to use fructose and *N*-acetyl-glucosamine (NAG), but not glucose [18]. Some mutants developed from the just-mentioned wild-type strain (i.e., G^+1, $H1G^+3$) turned out to be capable of utilizing glucose [35]. Recently, Raberg et al. [32, 33] reported that the mutant *R. eutropha* G^+1 transports glucose in the cell by the action of *N*-acetyl-glucosamine phosphotransferase system (NAG-PTS). Surprisingly, after the import into the cell accomplished by the NagE protein, the intracellular phosphorylation of glucose seems to be mediated by glucokinase (GLK, E.C. 2.7.1.2), and not by the NagF proteins (cytosolic component of PTS). Furthermore, genome sequencing of *R. eutropha* H16 (*C. necator*) [27] has confirmed that *R. eutropha* H16 does not possess 6-phosphofructokinase (PPK, E.C. 2.7.1.11) encoded by the *pfk* gene. Thus, fructose-6-phosphate (F6P) is not converted into fructose-1,6-bisphosphate (FBP) through the Embden–Meyerhof–Parnas (EMP) pathway. The Entner–Doudoroff (ED) pathway is dominant in hexoses degradation, hence the major part of the C-flux in *R. eutropha* H16, a strain from which the mutant *C. necator* DSM 545 was developed, enters the EMP at glyceraldehyde-3-phosphate (G3P) and pyruvate nodes, and 6-phosphogluconate (6-PG) is an intermediate. If essential genes encoding the ED pathway are "knocked out", considerable retardation of cell growth on D-fructose occurs. It is noteworthy that the key enzyme responsible for supplying the oxidative pentose phosphate pathway (PPP), namely 6-phosphogluconate dehydrogenase (6-PG DH, E.C. 1.1.1.44), was not detected in *R. eutropha* H16; moreover, there is no evidence for the related gene; contrariwise, the genes responsible for the anabolic EMP pathway (gluconeogenesis) do exist [27]. In order to undergo catabolism, glycerol as the sole carbon source must be transported across the cytoplasmic membrane by facilitated diffusion (mediated by the facilitator protein GlpF [39]). It seems that glycerol is thereafter subjected to phosphorylation by glycerol kinase (GLYK, E.C. 2.7.1.30) and subsequently to oxidation by glycerol-3-phosphate dehydrogenase (GLY-3-P DH, E.C. 1.1.1.94). The presence of glucose in growth medium causes lowered (or interrupted) glycerol consumption by *C. necator*. This is due to the fact that glycerol metabolizing enzymes, i.e., GLYK and GLY-3-P DH, are subjects of inhibition by EMP substrates. FBP inhibits GLYK, and GLY-3-P DH is inhibited by PEP, dihydroxyacetone phosphate (DHAP) as well as 3-phosphoglycerate. To overcome the problem of slow growth and modest PHB synthesis rate by *C. necator* on glycerol, metabolic engineering methods could be applied. The first step in such a complex work is the analysis of the existing metabolic state when *C. necator* grows and synthesizes PHB on glycerol. The key enzyme for the glycerol degradation in *C. necator* DSM 545 (a $H1G^+3$ mutant) is GLY-3-P DH. This enzyme was not studied for *C. necator* in details. For example, it is not yet known if NAD/NADH or FAD/$FADH_2$ coenzymes are included in this reaction. The availability of the mentioned reduced coenzymes is a well-known key factor in PHB synthesis. Grousseau et al. [12] have demonstrated how growth controls generation and availability of NADPH, as well as the resulting impact on PHB yields and kinetics. Furthermore, the genome sequence of strain *C. necator* DSM545 is still not available, hence, it is not clear if this strain possess 6-PG DH or not (in *C. necator* N1, investigated by Pöhlein et al. [29], three genes for coding this enzyme were found with the subsequent LocusTags: CNE_BB2p02120; CNE_BB1p11870, and CNE_BB1p13160 IMG/), whereas in *R. eutropha* G^+1 corresponding genes were not detected [30].

The aim of this work is to analyze (experimentally and in silico) the metabolic situation of *C. necator* DSM 545 growing on glycerol, concerning both growth and PHB synthesis phase. For that purpose, the mathematical modeling of metabolic network using elementary flux modes and yield space analysis was applied. Special attention was devoted to possible metabolic and genomic variations concerning GLY-3-P DH and coenzymes (i.e., NAD, FAD), the presence of 6-PG DH as well as the role of the anabolic EMP pathway (gluconeogenesis).

Metabolic network modeling and mathematical simulation of metabolic networks are useful tools for getting deeper insights into molecular mechanisms and physiology of a particular organism. The reconstruction of metabolic networks

is based on genome structure. For a particular organism, the reconstruction involves collecting all relevant metabolic data by searching through different databases, such as GeneDB, Kyoto Encyclopedia of Genes and Genomes (KEGG), BioSilico, University of Minnesota Biocatalyst/Biodegradation Database (UMBBD), Transport DB, ExPASy, BRENDA, and IMG. Because of frequently occurring discrepancies between data concerning a particular organism originating from enzyme, gene, kinetic and reaction databases, the verification of metabolic network is necessary. The reconstruction with verification includes a systematic approach to data compilation (originated from various sources) and clarification of all existing discrepancies. Methods of metabolic engineering and its practical applications were summarized earlier by Stephanopoulos et al. [45] as well as by Gombert and Nielsen [11]. Some improvements of existing methods as well as new approaches in this field have been developed recently. They are focused on analysis of complex metabolic networks concerning their usage in different subfields of bio-science. For this purpose, the pathway representations in metabolic network approaches are developed as follows: extreme pathways approach [24, 25, 31], minimal metabolic behaviors [19], elementary (flux) mode analysis [36, 37, 44], and flux balance methods based on linear programming such as flux coupling analysis [2], flux balance analysis [7, 23, 46], flux variability analysis [3, 13, 22, 26]. In addition, the dynamic simulation and parameter estimation methods are often applied [6]. Extreme pathways are defined as convex basis vectors consisting of metabolic steady-state functions. Any metabolic network contains a unique set of extreme pathways. Flux balance analysis tends to reach only a single solution by means of optimization of the objective function (e.g., concentration, yield, or specific growth rate) and can extract the most effective pathway through the metabolic network. Flux variability analysis (FVA) is a useful tool for investigating changes in metabolic flux distribution under several perturbed conditions [26]. The "minimal metabolic behaviors" (MMBs) approach based on non-negativity constraints sets delivers a complete description of the flux cone. MMBs are uniquely determined by the applied network. Dynamic simulation and parameter estimation method uses an ordinary differential equation system able to calculate the rates of change in whole space of metabolites' concentrations.

Elementary modes (EMs) are defined as a set of vectors originated from the stoichiometric matrix of a metabolic network, and have three main properties:

1. Unique set of elementary modes exists for a given network;
2. "Non-decomposability" or "genetic independence" means that a minimal number of reactions is needed to exist as a functional unit to be an elementary mode. Any removed reaction in any elementary mode leads to the consequence that the whole elementary mode cannot operate as a functional unit;
3. All routes through a metabolic network consistent with property (2) are parts of elementary modes set.

EMs display the smallest sub-networks that allow a metabolic reconstruction network to operate under steady-state conditions. According to Stelling et al. [44], when evaluating whether some metabolic routes are suitable for the representation of set of enzymes (metabolic pathway) or not, stoichiometry and thermodynamics must be taken into account.

The possible combinatorial explosion of a number of EMs in complex networks could limit this approach. In such cases, a reduction of a set of EMs using "yield analysis" (YA) is an appropriate method for extracting the minimal subset of EMs that is able to describe a real metabolic situation [42]. The solution space in yield analysis of metabolic pathways is a bounded convex hull in the yield space. After application of high structured mathematical models and elementary modes with yield analysis for analyzing the five-step continuous production of PHB on glucose by *C. necator* [21], the combined elementary modes method with perturbed metabolic conditions and yield analysis was applied in work at hand in order to study the metabolic network of *C. necator* DSM 545 that produces polyhydroxyalkanoates (PHAs) while growing on glycerol. The target was to investigate the possibilities for the metabolic improvement of this strain in PHB production on waste glycerol from biodiesel production.

Materials and methods

Microorganism and medium

The organism used in this study was *C. necator* DSM 545, which can grow on glucose, fructose, and glycerol as the sole carbon sources and is able to synthesize a low amount of PHB in the exponential growth phase and an increased quantity of PHB in the nitrogen limited/C-sufficient non-growth phase. It was obtained from DSMZ (Deutsche Sammlung von Mikroorganismen und Zellkulturen GmbH), Braunschweig, Germany, as vacuum-dried culture. The strain was revitalized and cultivated using the medium that contains (per liter): Na_2HPO_4, 7.17 g; KH_2PO_4, 3 g; $MgSO_4{\cdot}7H_2O$, 0.2 g; $(NH_4)_2SO_4$, 1 g; $CaCl_2{\cdot}2H_2O$, 0.02 g; NH4Fe(III)citrate, 0.05 g; trace element solution SL6, 1 mL; glycerol, 10 g. The trace element solution SL6 was composed as follows (per liter): $ZnSO_4{\cdot}7H_2O$, 100 mg; H_3BO_3, 300 mg; $CoCl_2{\cdot}6H_2O$, 200 mg; $CuSO_4$, 6 mg; $NiCl_2{\cdot}6H_2O$, 20 mg; $Na_2MoO_4{\cdot}2H_2O$, 30 mg; $MnCl_2{\cdot}2H_2O$, 25 mg.

Analytical procedures

Determination of cell dry mass (CDM)

A gravimetrical method was used to determine the biomass concentration expressed as CDM in fermentation samples. Five milliliters of culture broth was centrifuged in pre-weighed glass screw-cap tubes for 10 min at 10 °C and 4,000 rpm in a Heraeus Megafuge 1.0 R refrigerated centrifuge. The supernatant was decanted and used for substrate analysis. The cell pellets were washed with distilled water, re-centrifuged, frozen, and lyophilized to a constant mass. CDM was determined as the mass difference between the tubes containing cell pellets and empty tubes. The determination was done in duplicate. The lyophilized pellets were subsequently used for determination of intracellular PHB as described below. Residual biomass (non-PHB part of biomass) was calculated by subtracting of PHB mass from CDM mass.

GC-FID analysis of PHB

PHB in lyophilized biomass samples was transesterificated by acidic methanolysis according to Braunegg's method [1]. Gas chromatographic analysis was performed with a 6850 Network GC System (Agilent Technologies), equipped with a 25 m × 0.32 mm × 0.52 μm HP5 capillary column and a flame ionization detector (FID). Helium (Linde; purity = 4.6) was used as a carrier gas with a split-ratio of 1:5, hydrogen (Linde; purity = 5.0) and synthetic air (Linde; purity = "free of hydrocarbons") as detector gases and nitrogen (Linde; purity = 5.0) as auxiliary gas.

The following protocol for the temperature program was used: Initial temperature: 50 °C; rate 1:15 °C/min; final temperature 1:60 °C; rate 2:2 °C/min; final temperature 2:80 °C; final temperature 3:300 °C; final time 3:5 min. The determination of all samples was done in duplicate. The methyl esters of PHB constituents were detected by a flame ionization detector (FID); carrier gas: helium (split-ratio of 1:10), injection volume of 1 μL. The co-polyester Poly(3HB-*co*-15.6 %-3HV) (BIOPOL, ICI, UK) was used as reference material and hexanoic acid acted as the internal standard. The PHB content (wt %) was defined as the percentage of PHB concentration to dry cell mass (CDM).

Ammonia determination

A commercially available test (Merck, Spectroquant, 1.00683.0001) was used following the principle of ammonia reacting with hypochlorite ions to monochloramine, which further reacts with substituted phenol to form a blue indophenol derivative. This complex can be determined photometrically at 690 nm using a Genesys 10S UV–Vis Spectrophotometer (Thermo Scientific, USA). The measuring range of the test for ammonium is 6–193 mg/L. Ammonium sulphate was used as reference. Deionized water was used as zero reference.

Glycerol determination

Glycerol concentration in supernatant (remaining after the centrifugation step described in 2.2.1) was monitored using a high-performance liquid chromatography (HPLC; *Shimadzu*) equipment consisting of a thermostated Aminex HPX 87H column (thermostated at 75 °C, Bio-Rad, Hercules, CA, USA), a LC-20AD pump, a SIC-20 AC autosampler, a RID-10A refractive index detector, and a CTO-20 AC column oven. For registration and evaluation of the data, LC solution software was used. Sterile-filtrated supernatant was transferred into vials and water was used as eluent at a flow rate of 0.6 mL/min. External standards were prepared using different concentrations of p.a. glycerol.

Cultivation conditions

Inoculum preparation

Colonies from solid agar slants (2.1) were cultivated in small baffled shaking flasks (100 mL medium in 300-mL flasks) at 37 °C under continuous shaking in liquid minimal media containing glycerol as the sole carbon source. After sufficient growth of the strain was achieved, large baffled shaking flasks (1 L) containing fresh medium (250 mL) were inoculated with each 5 mL of the first liquid cultures. These large cultures were incubated overnight under continuous shaking at 37 °C and subsequently used as inoculum cultures for the bioreactor experiment.

Cultivation in bioreactor

The cultivation was carried out aerobically in a laboratory bioreactor (Labfors 3, Infors, CH, working volume 5 L; glass vessel stirred from the upper side) under controlled conditions for pH value (7.1 ± 0.1), temperature (37 °C), and dissolved oxygen concentration pO_2 (controlled by agitation speed of two axial stirrers and air flow rate; during growth phase, pO_2 amounted to 40 %, during the phase of predominant PHB-accumulation to 20 % of the oxygen saturation concentration). The sterilization of the reactor equipment and the relevant accessories (feed bottles, nutrients) was accomplished via heat sterilization in an autoclave. All relevant cultivation parameters (pH value, temperature, pO_2) as well as the addition of substrate feed, pH-value correcting agents, antifoam agent, etc., were monitored automatically using INFORS IRIS software version 5.

An amount of 2.5 L of a minimal medium containing the double concentration for all ingredients as described for inoculum preparation (2.3.1) was inoculated with the same volume of the dense inoculum cultures (ca. 4 g/L) of *C. necator* (2.3.1).

The pH value was kept constant by automatic supply of aqueous NH_4OH solution (25 %) that, at the same time, kept the concentration of the nitrogen source NH_4^+ at a constant level. After a desired concentration of biomass (20 g/L; $t = 20$ h) was obtained, the NH_4OH solution was exchanged by aqueous NaOH solution (20 %) in order to achieve restricted concentrations of nitrogen to provoke the stop of biomass growth and the shift of carbon flux towards PHB accumulation.

After the fermentation stoppage ($t = 30$ h), the cells were in situ pasteurized by heating to 70 °C for 20 min, centrifuged (Sorvall RC-5B Refrigerated Superspeed centrifuge), frozen, and lyophilized for 48 h (Lyophilisator Christ Alpha 1-4 B, Germany). The resulting dry biomass was used for product (PHB) recovery.

Experimental yield estimation

Time range of exponential growth phase was determined from relation:

$$\ln (X_r/X_{ro}) = f(t) \quad (1)$$

where X_r and X_{ro} are the residual biomass concentrations (non-PHB part of CDM) at the end and at the beginning of straight line achieved by linear regression. "t" designates the elapsed fermentation time in the bioreactor.

Residual biomass yield was calculated by

$$Y_{BIO/GLY} = \Delta X_r/\Delta GLY \quad (2)$$

and related product yield was calculated from relation

$$Y_{PHB/GLY} = \Delta PHB/\Delta GLY \quad (3)$$

where Δ means the difference of residual biomass, PHB, and glycerol concentration, respectively (related to time interval of straight line).

In silico calculations

Metabolic model

Basic formulations Relevant metabolic and transport data for building the metabolic network of regulated reactions for *C. necator* were retrieved by searching following databases: GeneDB, KEGG, BioSilico, UMBBD, Transport DB, ExPASy, BRENDA, and IMG. In addition, some data concerning transport equations published in scientific articles by Pohlmann et al. [30] and Raberg et al. [32, 33] were included as well as data from the works of Franz et al. [9], Park et al. [27], Pöhlein et al. [29], and Grousseau et al. [12]. The resulting metabolic network is presented in Fig. 1. It contains roughly the phosphoenolpyruvate-sugar transpherase system (PTS), glycerol metabolizing enzymes, ED, PPP, tricarboxylic acid (TCA) and glyoxylate (GOXC) cycles, PHB synthesis, and degradation pathways.

Equations of reactions that are related to the above metabolic network are summarized in Online Resource 1 "ESM 1.doc" with indicated referent direction.

The state of the metabolic system is defined by biomass concentration, by vector of concentrations of external biochemical species (substrates and products), and by vector of internal biochemical species concentrations. Glucose, glycerol, oxygen, and ammonia were considered in this work as external substrates, while CO_2, PHB, and the new grown non-PHB part of biomass were external products. From the biological point of view, PHB constitutes an intracellular storage material, but, due to the requirements of the mathematical procedure, it was extraordinarily treated as a separate compartment, namely "extracellular" product (i.e., "extracellular" with regard to the non-PHB part of biomass).

Mass balance equations for the established metabolic network are presented in Online Resource 2 (ESM 2.doc). The matrix with stoichiometric coefficients of internal metabolites in case when NAD and NADH are reactants in reaction of GLY-3-P DH is presented as Online Resource 3 (Matrix A_NAD; ESM 3.xls); the matrix with stoichiometric coefficients of internal metabolites in case when FAD and FADH are reactants in reaction of GLY-3-P DH is presented as Online Resource 4 (Matrix A_FAD; ESM 4.xls), and the matrix with stoichiometric coefficients of external species is given as Online Resource 5 (Matrix B; ESM 5.xls).

Elementary mode concept The presented metabolic network (Fig. 1) was analyzed by the elementary flux modes analysis method described earlier [36, 37]. For the purpose of this work, it was assumed that all concentrations of internal metabolites are in quasi-steady state, e.g.,

$$dC_i/dt = 0 \quad (4)$$

(it is reasonable to keep this assumption valid for exponential growth and for the *N*-limited non-growth PHB synthesis phase) so that all right sides of balance equations related to the internal metabolites are equal to zero. This way, the set of mass balance equations for internal metabolites becomes linear, so the system could be solved and relative metabolic fluxes can be calculated by using standard software for metabolic flux analysis of cellular networks. In this work, the program Metatool, version 5.1 was used. This software was originally developed by Pfeiffer et al. [28] and further advanced by von Kamp and Schuster [47].

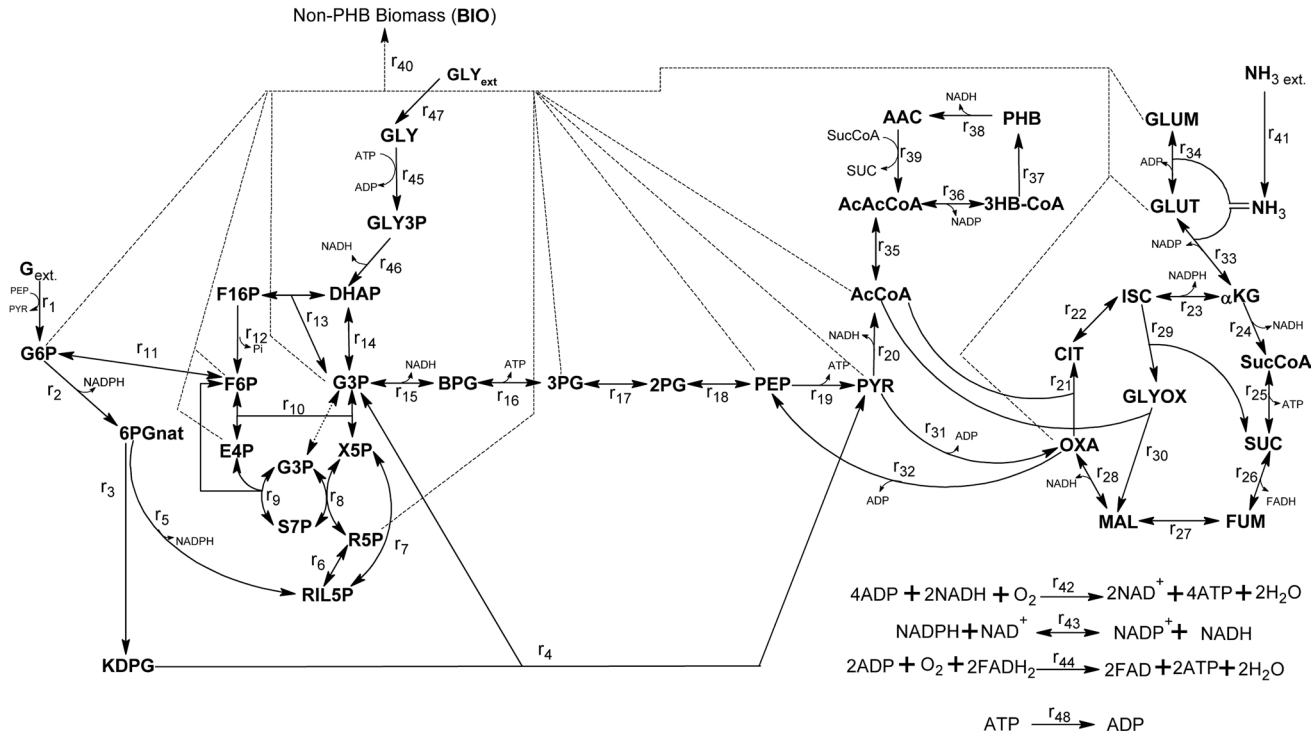

Fig. 1 Metabolic network of *C. necator* for growth on glucose and glycerol

The total set of EMs obtained by Metatool was reduced afterwards to a smaller set applying the "metabolic yield analysis" method described by Song and Ramkrishna [42] and by Song et al. [41]. A reduced set of EMs was obtained under the following assumed conditions:

- the metabolic network is able to produce new non-PHB biomass or PHB or simultaneously both of them,
- PHB degradation does not occur if a sufficient carbon source is present (r_{38} and r_{39} fluxes were set to zero),
- in case of growth on glycerol as the sole carbon source, the flux of PTS (r_1) was set to zero,
- 6-PG DH was considered alternatively (i.e., $r_5 > 0$ and $r_5 = 0$),
- coenzymes for GLY-3-P DH (i.e., NAD and FAD) were considered alternatively.

The basic idea of metabolic yield analysis is to project EMs from flux space onto yield space. This can be accomplished by normalizing stoichiometric coefficients of overall reaction of each elementary mode with respect to a reference substrate. If glycerol is taken as the reference substrate, the elementary modes can be represented in four-dimensional yield space ($Y_{BIO/GLY}$, $Y_{PHB/GLY}$, $Y_{GLU/GLY}$, $Y_{N/GLY}$). However, the dimensionality of this yield space can be reduced. Namely, in this study the microorganism grows only on glycerol, hence the dimension $Y_{GLU/GLY}$ can be excluded. In addition, due to the fact that residual biomass is experimentally as well as stoichiometrically correlated to the consumed nitrogen source, the dimension $Y_{N/GLY}$ can also be excluded. As a result, our yield space has only two dimensions ($Y_{BIO/GLY}$, $Y_{PHB/GLY}$). The calculated yields of PHB and residual biomass concerning a reduced set of EMs were used for obtaining a convex hull in the ($Y_{BIO/GLY}$, $Y_{PHB/GLY}$) yield space. These yields were compared to experimental data using the Euclidean distance. The experimental data are represented as a linear combination of elementary modes with each mode having been assigned a weighting factor. A unique solution is obtained by the method of quadratic programming described in [38], which favors the modes that are closest to the actual state of system as biologically most relevant (thus assigning greater weights to closer modes). In the extended version of investigation, all possible combinations between EMs from the reduced set were generated and scrutinized in order to give the same yields as obtained in the experiment.

Flux distribution under perturbed metabolic conditions

For growth on glycerol, metabolic flux distributions under perturbed metabolic conditions were investigated using the established metabolic network (Fig. 1). Metabolic fluxes were calculated with the basic presumption that PHB can be synthesized already in the growth phase. Under this

basic condition, calculations were performed by script written in "Matlab" software, assuming some different metabolic situations as follows:

Case (1): the pair NAD/NADH was assumed to participate in the activity of GLY-3-P DH. All possible EMs from reduced set (188) that satisfy basic condition were included in the calculation in order to achieve the same yields as in the experiment;

Case (2): as in case (1), NAD and NADH were supposed to be the reactants in reaction of GLY-3-P dehydrogenase. Assuming basic condition, C-flux was in silico-directed towards the G3P node in the EMP pathway (that means, the flux rate of GA-3-P DH is greater than the flux rate of anabolic EMP pathway (gluconeogenesis, opposite direction than fructose-1-6-bisphosphate aldolase (FBPA, EC 4.1.2.13) reaction in normal glycolysis); $r_{15} > r_{13}$;

Case (3): the pair NAD/NADH was again supposed to be included in the reaction catalyzed by GLY-3-P DH and the rate of anabolic EMP pathway was assumed to be greater than rate of glyceraldehyde-3-phosphate dehydrogenase (GA-3P DH, EC 1.2.1.12) ($r_{13} > r_{15}$), hence the adjacent pathway towards F6P (and further towards glucose-6-phosphate) supply substrates for the ED;

Case (4): ED dominates the EMP pathway ($r_4 > r_{15}$; 2-dehydro-3-deoxy-phosphoglucanate aldolase (PGA, E.C. 4.1.2.14) flux is greater than the flux of GA-3P DH, so the major amount of pyruvate in the cell is produced through r_4). As above, GLY-3-P dehydrogenase was assumed to use the pair NAD/NADH in the reaction.

Cases (5), (6), (7), and (8) were the same as (1), (2), (3), and (4), respectively, except the pair FAD/$FADH_2$ (instead of NAD/NADH) was assumed to participate in GLY-3-P dehydrogenase reaction. For these cases, the reduced set of EMs includes 165 EMs.

Cases (9–16) were the same as (1–8) except that the reaction r_5 is excluded from calculation (i.e., its flux value always equals zero). For the cases (9–12), NAD/NADH as reactant/product pair was involved in GLY-3-P DH reaction, and the number of combined EMs was 65. In addition, for the cases (13–16), the pair FAD/$FADH_2$ was a part of GLY-3-P DH system and the number of EMs was 61.

Metabolic fluxes for the cases (17) and (18) were calculated for such EMs, where the yields were closest to the experimental result in the yield space according to the Euclidean distance method. These two cases differ in NAD/NADH or FAD/$FADH_2$ as participants in system of GLY-3-P DH.

Results and discussion

Two main types of waste substances originated from biodiesel production were investigated for PHA production in the past: fatty acid esters by Vrana Špoljarić et al. [49], and glycerol [4, 10, 14, 48]. Glycerol is the typical carbon source that can be metabolized by microorganisms through sugar-degrading pathways, but it must be phosphorylated and oxidized to DHAP. In such a case, gluconeogenesis is essential in order to provide sugar phosphates as anabolic precursors. The key enzyme for DHAP synthesis from GLY-3-P is GLY-3-P DH, which is not investigated in detail for *C. necator*. A lot of microbes possess NAD-dependent GLY-3-P dehydrogenase, but in some of these microbes, the FAD-binding membrane-bound respiratory enzyme is present (e.g., *E. coli* K-12 cultivated under aerobic conditions). NADH as product of the GLY-3-P oxidation can be the source for NADP reduction catalyzed by the action of transhydrogenases, and NADPH is the essential protone donor for PHB synthesis. Otherwise, if FAD is assumed to be the reactant for GLY-3-P DH, the ATP generation in respiratory chain will be supplied. Both mentioned metabolic hypotheses were the subject of testing in the work at hand. The key enzymes fructose-1,6-bisphophatase, FBPA, and 6-PG DH are lacking in wild-strain and in G^+1 mutants of *C. necator* [30, 32, 35], so the EMP and the PPP are incomplete and the ED pathway is the main sugar-degrading route. Interestingly, the mutant *C. necator* N1 possess three genes for 6-PG DH [29], so it was appropriate to test both possibilities (concerning our strain *C. necator* DSM 545 [$H1G^+3$ mutant], 6-PG DH expression, and its impact on PHB synthesis).

Complementary modeling and experimental approach was used by Grousseau et al. [12] to explore how growth controls the NADPH generation, PHB yields, and the kinetics, when *C. necator* uses organic acids as carbon source. Results of this issue were surprising: the anabolic demand allowed the NADPH production through the ED pathway with a high theoretical PHB yield of 0.89 mol C (mol C)$^{-1}$. Interestingly, without biomass production, NADPH regeneration was only possible from the isocitrate dehydrogenase (IDH, E.C. 1.1.1.42) action with a theoretical yield of 0.67 mol C (mol C)$^{-1}$. The maximal specific NADPH production rate was achieved at maximal growth rate and it was found to be pivotal to achieve the maximal PHB production rate. NADPH consumed by the PHB synthesis reaction must be generated somewhere in the metabolic network, and four candidates were underlined by the mentioned authors:

1. glucose-6-phosphate dehydrogenase of the ED,
2. IDH of the TCA cycle,
3. NADP-malic enzyme (E.C. 1.1.1.40),
4. transhydrogenases.

Two genes (*icd1* and *icd2*) encoding for IDH were identified by Wang et al. [50], and two IDHs with affinity to

both NAD^+ (E.C. 1.1.1.41) and $NADP^+$ (E.C. 1.1.1.42) were separated and purified. In addition, by sequence analysis of *C. necator*, an additional gene coding for an IDH (icd3/locus H16_B1016) was identified by Pohlmann et al. [30].

For glycerol as the sole carbon source, the general metabolic situation is similar as for growth on organic acids, i.e., the anabolic EMP should provide sugar phosphates as growth precursors. Considering all these facts, both NAD and FAD from GLY-3-P DH could significantly change the metabolic situation concerning NADPH synthesis, thus severely impacting PHB production when *C. necator* uses glycerol as the sole C-substrate.

During cultivation of *C. necator* DSM 545 on glycerol as the sole carbon source applied in this work, two different cultivation phases can clearly be distinguished:

1. the exponential phase characterized by exponential biomass growth combined with limited PHB synthesis, and
2. non-growth, nitrogen-limited phase of predominant PHB synthesis.

During exponential growth, yield coefficients for biomass ($Y_{BIO/GLY}$) and for PHB ($Y_{PHB/GLY}$) of 0.388 g g^{-1} and 0.154 g g^{-1}, respectively, were achieved. These values were used as reference values for comparison with in silico calculated yields.

Under supposed intracellular steady-state conditions for exponential phase of growth, the metabolic network presented in Fig. 1 has resulted in 2,722 elementary modes calculated with the software package Metatool. This result was obtained under the assumption that glucose and glycerol act as carbon sources and that the pair NAD/NADH is involved in the reaction catalyzed by GLY-3-P DH. If, under the same conditions, instead of NAD/NADH, the pair FAD/$FADH_2$ is assumed to act as reactants of the GLY-3-P dehydrogenase system, the total number of elementary modes amounted to 2,701. When the fluxes through the PHB-degrading reactions (r_{38} and r_{39}; Fig. 1) were set to zero (this is valid at sufficient concentration of carbon source in the culture medium), and when glycerol was regarded as the sole carbon source (i.e., $r_1 = 0$), as well as assuming that NAD/NADH are reactants in the reaction catalyzed by GLY-3-P DH, 202 elementary modes were detected. Among these 202 elementary modes, 188 were related to a synthesis of catalytically active biomass (non-PHB part), to PHB, and to synthesis of both of them simultaneously. Only 43 modes represented the last case of simultaneous production of PHB and non-PHB part of biomass (residual biomass). Under the same conditions (i.e., r_1, r_{38}, and $r_{39} = 0$) but with FAD/$FADH_2$ involved in the GLY-3-P DH reaction,

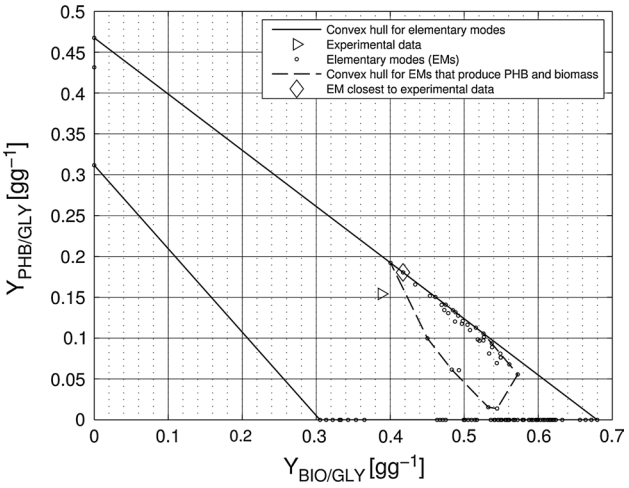

Fig. 2 Yield space of elementary modes for growth of *C. necator* on glycerol when the pair NAD/NADH is supposed to be involved in reaction of GLY-3-P DH. *Dashed hull* denotes reduced yield space concerning EMs with simultaneous synthesis of biomass and PHB

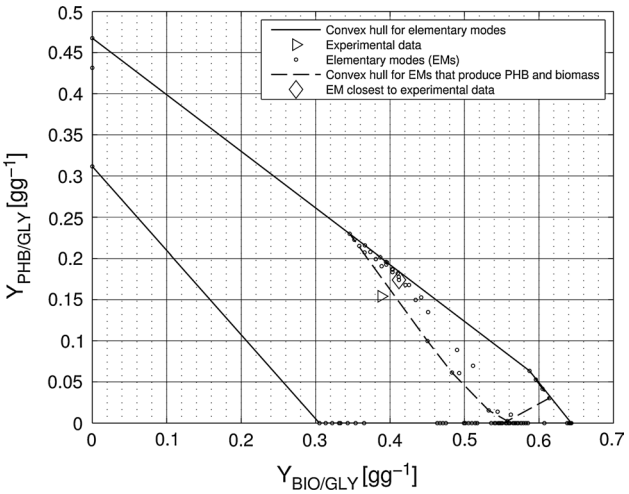

Fig. 3 Yield space of elementary modes for growth of *C. necator* on glycerol when the pair FAD/$FADH_2$ is supposed to be involved in the reaction of GLY-3-P DH. *Dashed hull* denotes additionally reduced yield space concerning EMs with simultaneous synthesis of biomass and PHB

179 elementary modes were detected; among them 165 have been related to synthesis of new residual biomass (non-PHB part), to PHB and to both processes simultaneously, but only 36 of them represented simultaneous production of PHB and non-PHB part of biomass. For reduced sets of elementary modes (188 from 2,722, and 165 from 2,701), related yields of non-PHB biomass ($Y_{BIO/GLY}$) and PHB ($Y_{PHB/GLY}$) were calculated with the Metatool software. These yields are represented in Figs. 2 and 3.

Triangles in yield space in Figs. 2 and 3 represent the experimental yield results achieved for growth phase of *C. necator* on glycerol as carbon source. Diamond shapes in these figures indicate those EMs that are closest to the corresponding experimental result (concerning Euclidean distance between experimental and simulated results). In both Figs. 2 and 3 it can be seen that none of the points in the yield space exactly coincides with experimental result. Moreover, experimental yields did not fall in the reduced yield space of EMs limited by the condition that biomass and PHB are synthesized simultaneously (dashed convex hull). Based on the facts described above, it is clear that no single EMs (or no linear combination of EMs that "synthesizes" biomass and PHB simultaneously) exist that exactly represent the current experimental situation. This is the reason for obtaining the solution by combining EMs from yield space in a way that the weighting factors are assigned to them as a measure of their influence.

Regarding NAD or FAD as cofactors for GLY-3-P DH and concerning presence/absence of 6-PG DH as well as the activity of different sugar degrading pathways (e.g., EMP, ED), resulting metabolic fluxes (calculated by help of elementary modes and yield space analysis) are presented in Figs. 4, 5, and 6.

Prior to analysis of metabolic fluxes, it was necessary to test if all investigated metabolic situations (cases 1–16) can reach the experimental yields when *C. necator* grew on glycerol. Although it was hoped that such testing will exclude some cases (1–16), this was not the case. All tested metabolic situations were able to reach experimental yields. To ensure that results for metabolic situations (cases 1–16) will be clearly and comprehensively presented, tables with relative fluxes were prepared (Table 1 for r_5 included and Table 2 for r_5 excluded).

Three different categories of metabolic fluxes are marked in the tables presented above according to following quantitative criteria:

- group of fluxes that deviate from basic reference value for +50 % or more;
- group of fluxes that deviate from basic reference value −50 % or more but do not change their direction;
- group of fluxes related to reactions that have changed their direction (fluxes with minus sign).

Results in Figs. 4, 5, and 6 can be discussed by help of data from Tables 1 and 2 from three different points of view:

- the first one is the possible difference between metabolic fluxes obtained if GLY-3-P DH is assumed to use NAD/NADH or FAD/$FADH_2$;
- the second one is the difference in results when the presence or absence of the enzyme 6-PG DH (r_5) is taken into consideration;
- the third one is the possible effect of alternative metabolic routes (EMP and ED) on metabolic fluxes.

Influence of NAD/NADH and FAD/$FADH_2$ as cofactors in GLY-3-P DH

According to results presented in Figs. 4, 5, and 6, it seems that some fluxes of metabolic routes were not altered, regardless of whether the NAD/NADH or FAD/$FADH_2$ were included in the reaction of GLY-3-P DH (i.e., glycerol consumption/r_{46}–r_{47}/, PHB synthesis/r_{35}–r_{37}/, and amino acid synthesis/r_{33}, r_{34}, r_{41}/). Contrariwise, fluxes of pentose phosphate, EMP, ED, and TCA pathways were slightly different (Fig. 4a; valid for cases with 6-PG DH included). An exception in PPP is reaction r_7 (R5PE) that was as well as reaction r_{44} (from respiratory chain) significantly increased when FAD is assumed to be the part of GLY-3-P DH reaction (Table 1). Remarkably, under the mentioned conditions, r_{43} (transhydrogenase) was reduced by ~35 % (Fig. 4a; Table 1) when r_5 was active, and changed direction when FAD was assumed to be the part of GLY-3-P DH without the presence of the 6-PG DH in metabolic network (Fig. 4b, Table 2).

Influence of presence/absence 6-PG DH

Regarding presence or absence 6-PG DH (r_5), it can be generally stated that, as expected, some PPP fluxes have changed their direction (r_7–r_9) when 6-PG DH is considered absent (Figs. 4, 5, 6b; Table 2), but the EMP (except pyruvate kinase r_{19} that was changed ~2.8 fold) as well as the TCA fluxes were slightly changed (Fig. 4b). Furthermore, the NAD(P)/NAD(P)H transhydrogenase (E.C. 1.6.1.1) (r_{43}) flux is very sensitive to change of all conditions when 6-PG DH is excluded from the reaction network, except when FAD acts as reactant with GLY-3-P DH.

Metabolic fluxes under perturbed metabolic conditions

Noteworthy results were obtained under perturbed metabolic conditions (Figs. 5, 6; Tables 1, 2). Results presented in these figures and tables lead to the conclusions that introduction of additional metabolic conditions (i.e., the dominance EMP or ED) caused (in silico) much more flux changes than the replacement of cofactors in the GLY-3-P DH reaction, or the presence/absence of 6-PG DH.

The next step in this work was to investigate how the perturbed metabolic conditions influenced the metabolic fluxes, assuming that the EMP pathway or the ED pathway are dominant when *C. necator* grows on glycerol. Glycerol

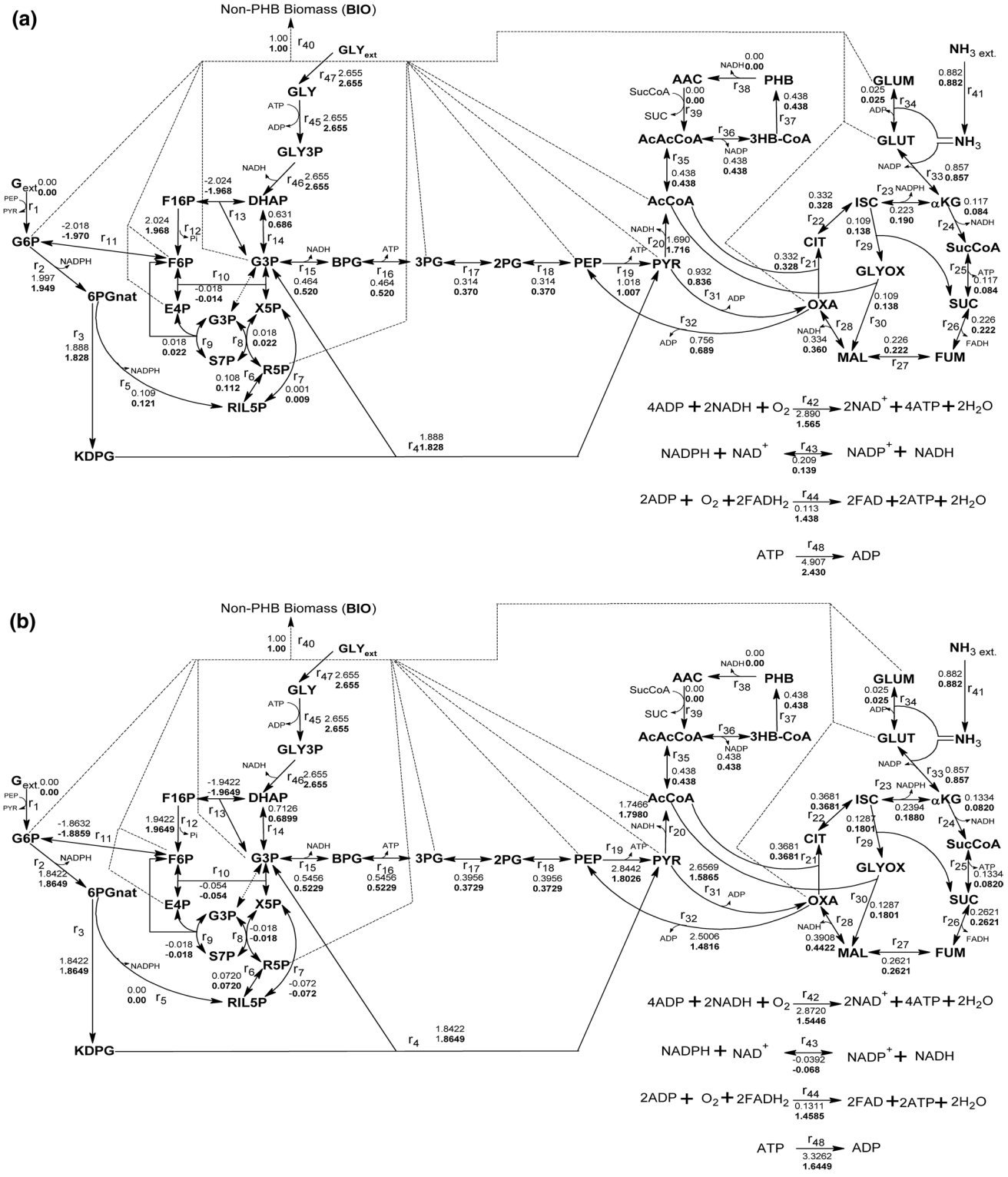

Fig. 4 Metabolic fluxes of *C. necator* resulted from combination of all EMs whose yields are in the yield space if NAD/NADH (*upper values*) or FAD/$FADH_2$ (*lower*, *bolded values*) were involved in reaction of GLY-3-P DH. 6-PG DH (r_5) included (**a**) and excluded (**b**) from metabolic network

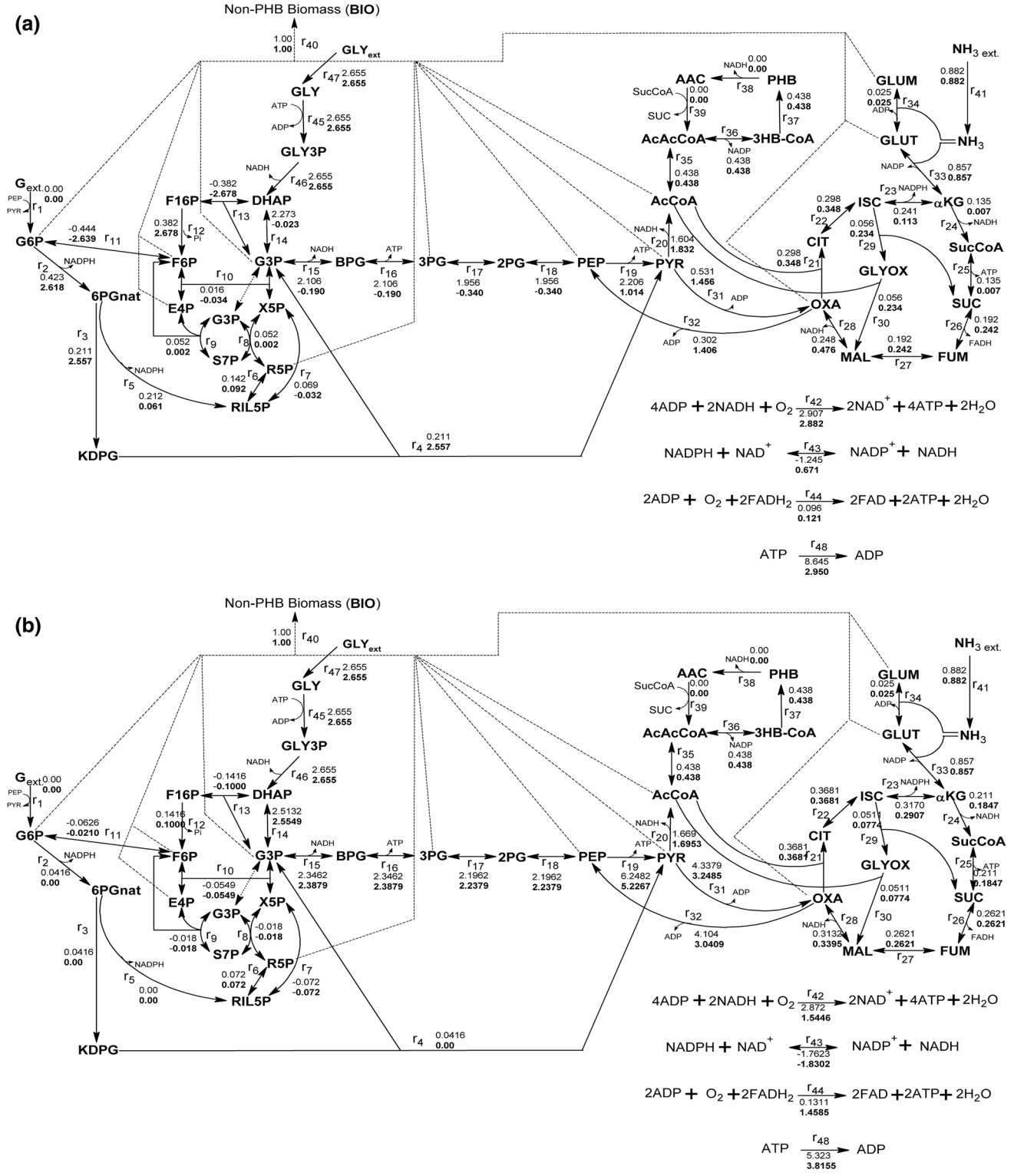

Fig. 5 Metabolic fluxes of *C. necator* resulted from situations where NAD/NADH (*upper values*) or FAD/FADH$_2$ (*lower*, *bolded values*) were involved in reaction of GLY-3-P dehydrogenase, achieved when EMP dominates over ED-pathway ($r_{15} > r_{13}$). 6-PG DH reaction (r_5) included (**a**) and excluded (**b**) from metabolic network

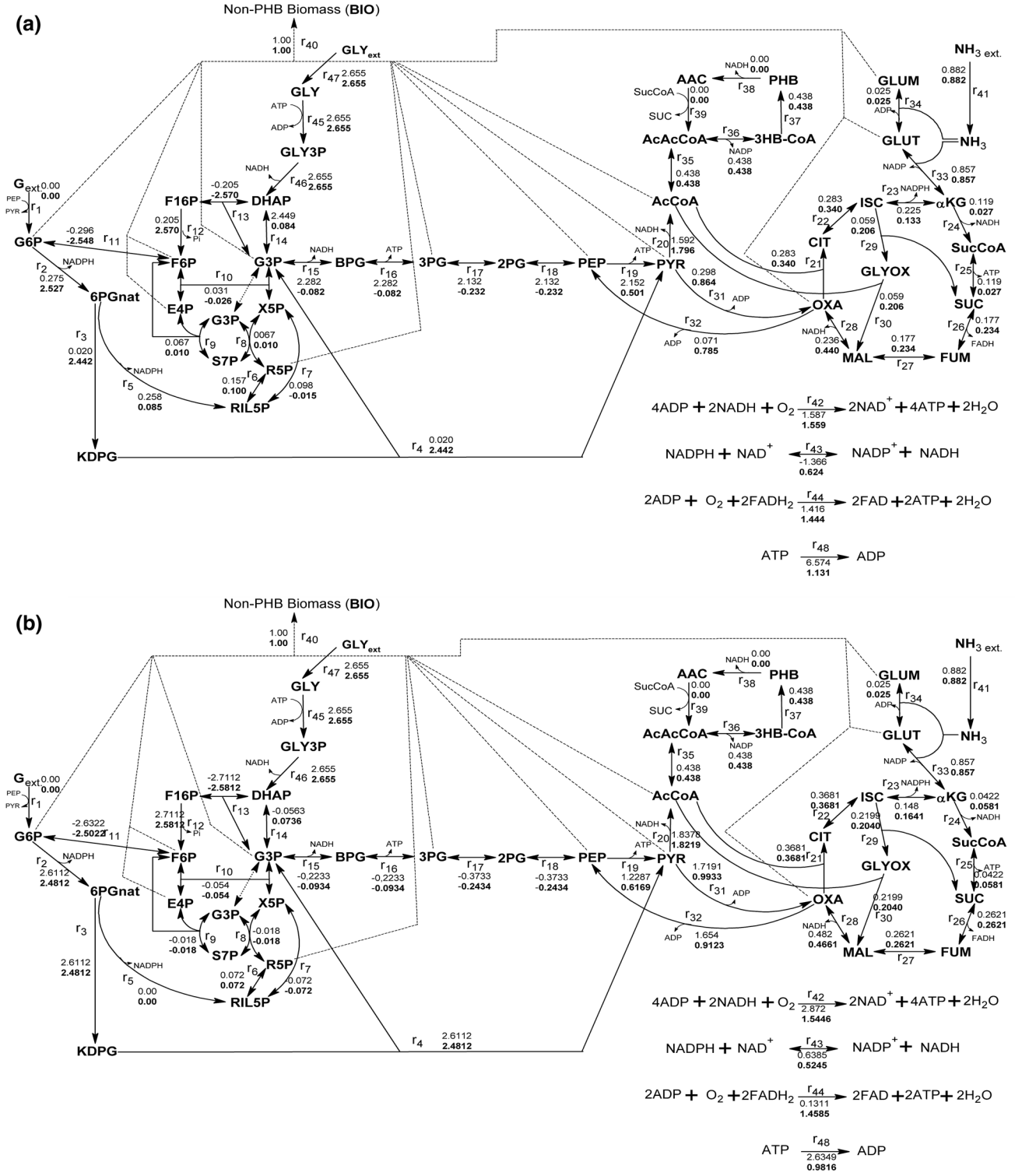

Fig. 6 Metabolic fluxes of *C. necator* resulted if NAD/NADH (*upper values*) or FAD/$FADH_2$ (*lower*, *bolded values*) were involved in reaction of GLY-3-P DH when ED-pathway dominates over EMP ($r_{13} > r_{15}$ and $r_4 > r_{15}$). **a** 6-PG DH reaction (r_5) included and **b** excluded from metabolic network

may enter the EMP pathway after transformation of Gly-3-P to DHAP and further to G3P. According to Steinbüchel [43] and Yu and Si [51], *C. necator* possesses a highly active ED pathway, thus it was reasonable to suppose that glycerol will be metabolized by two steps to DHAP that undergoes conversion towards (FBP) by the action of FBPA

Table 1 Relative flux values for different metabolic situations (cases 2–8) when the reaction r_5 is included into calculation

	Normalized fluxes with respect to case 1					
Reaction	Case 1	Case 2	Case 3 and 4	Case 5	Case 6	Case 7 and 8
r_1	0	–	–	–	–	–
r_2	1.9971	*0.2118*	1.3110	0.9760	*0.1378*	1.2653
r_3	1.8877	*0.1120*	1.3548	0.9684	*0.0109*	1.2936
r_4	1.8877	*0.1120*	1.3548	0.9684	*0.0109*	1.2936
r_5	0.1094	***1.9342***	0.5548	1.1079	***2.3282***	0.7761
r_6	0.1085	1.3134	0.8498	1.0359	1.4461	0.9244
r_7	0.0009	***76.7778***	**−35**	***9.7778***	***108.6667***	**−17.1111**
r_8	0.0185	***2.8378***	*0.1189*	1.2108	***3.6162***	0.5568
r_9	0.0185	***2.8378***	*0.1189*	1.2108	***3.6162***	0.5568
r_{10}	−0.0175	**−0.9429**	***1.9314***	0.7771	**−1.7657**	1.4686
r_{11}	−2.0181	*0.2200*	1.3077	0.9763	*0.1468*	1.2625
r_{12}	2.0242	*0.1887*	1.3228	0.9724	*0.1015*	1.2698
r_{13}	−2.0242	*0.1887*	1.3228	0.9724	*0.1015*	1.2698
r14	0.6307	***3.6038***	**−0.0362**	1.0885	***3.8836***	*0.1340*
r_{15}	0.4637	***4.5415***	**−0.4093**	1.1203	***4.9221***	**−0.1779**
r_{16}	0.4637	***4.5415***	**−0.4093**	1.1203	***4.9221***	**−0.1779**
r_{17}	0.3137	***6.2349***	**−1.0832**	1.1779	***6.7976***	**−0.7412**
r_{18}	0.3137	***6.2349***	**−1.0832**	1.1779	***6.7976***	**−0.7412**
r_{19}	1.0177	***2.1676***	0.9967	0.9891	***2.1143***	*0.4919*
r_{20}	1.6900	0.9490	1.0841	1.0151	0.9418	1.0627
r_{21}	0.3316	0.8975	1.0492	0.9882	0.8540	1.0247
r_{22}	0.3316	0.8975	1.0492	0.9882	0.8540	1.0247
r_{23}	0.2231	1.0807	0.5083	0.8498	1.0067	0.5979
r_{24}	0.1171	1.1537	*0.0632*	0.7139	1.0128	*0.2340*
r_{25}	0.1171	1.1537	*0.0632*	0.7139	1.0128	*0.2340*
r_{26}	0.2256	0.8493	1.0723	0.9827	0.7855	1.0363
r_{27}	0.2256	0.8493	1.0723	0.9827	0.7855	1.0363
r_{28}	0.3342	0.7424	1.4255	1.0766	0.7056	1.3172
r_{29}	0.1086	0.5203	***2.1593***	1.2716	0.5396	***1.9006***
r_{30}	0.1086	0.5203	***2.1593***	1.2716	0.5396	***1.9006***
r_{31}	0.9325	0.5690	***1.5619***	0.8965	*0.3192*	0.9262
r_{32}	0.7560	*0.3996*	***1.8599***	0.9115	*0.0943*	1.0385
r_{33}	0.8570	1	1	1	1	1
r_{34}	0.0250	1	1	1	1	1
r_{35}	0.4379	1	1	1	1	1
r_{36}	0.4379	1	1	1	1	1
r_{37}	0.4379	1	1	1	1	1
r_{38}	0	–	–	–	–	–
r_{39}	0	–	–	–	–	–
r_{40}	1.0000	1	1	1	1	1
r_{41}	0.8820	1	1	1	1	1
r_{42}	2.8903	1.0059	0.9972	0.5414	0.5491	0.5393
r_{43}	0.2087	**−5.9660**	***3.2166***	0.6665	**−6.5472**	***2.9919***
r_{44}	0.1128	0.8493	1.0718	***12.7509***	***12.5532***	***12.8041***
r_{45}	2.6549	1	1	1	1	1
r_{46}	2.6549	1	1	1	1	1
r_{47}	2.6549	1	1	1	1	1
r_{48}	4.9068	***1.7619***	0.6012	*0.4953*	1.3398	*0.2304*

The fluxes are normalized with respect to flux values in case 1

Change +50 % and more (*italics*); change −50 % and more (*bold italics*), change in direction (*bold*)

Table 2 Relative flux values for different metabolic situations (cases 10–16) when the reaction r_5 is excluded from the network (set to 0)

	Normalized fluxes with respect to case 9					
Reaction	Case 9	Case 10	Case 11 and 12	Case 13	Case 14	Case 15 and 16
r_1	0	–	–	–	–	–
r_2	1.8422	*0.0226*	1.4174	1.0123	0	1.3469
r_3	1.8422	*0.0226*	1.4174	1.0123	0	1.3469
r_4	1.8422	*0.0226*	1.4174	1.0123	0	1.3469
r_5	0	–	–	–	–	–
r_6	0.0720	1	1	1	1	1
r_7	−0.0720	1	1	1	1	1
r_8	−0.0180	1	1	1	1	1
r_9	−0.0180	1	1	1	1	1
r_{10}	−0.0540	1	1	1	1	1
r_{11}	−1.8632	*0.0336*	1.4127	1.0122	*0.0113*	1.3430
r_{12}	1.9422	*0.0729*	1.3959	1.0117	*0.0515*	1.3290
r_{13}	−1.9422	*0.0729*	1.3959	1.0117	*0.0515*	1.3290
r_{14}	0.7126	***3.5268***	**−0.0790**	0.9681	***3.5853***	*0.1033*
r_{15}	0.5456	***4.3002***	**−0.4093**	0.9584	***4.3766***	**−0.1712**
r_{16}	0.5456	***4.3002***	**−0.4093**	0.9584	***4.3766***	**−0.1712**
r_{17}	0.3956	***5.5516***	**−0.9436**	0.9426	***5.6570***	**−0.6153**
r_{18}	0.3956	***5.5516***	**−0.9436**	0.9426	***5.6570***	**−0.6153**
r_{19}	2.8442	***2.1968***	*0.4320*	0.6338	***1.8377***	*0.2169*
r_{20}	1.7466	0.9556	1.0522	1.0294	0.9706	1.0431
r_{21}	0.3681	1	1	1	1	1
r_{22}	0.3681	1	1	1	1	1
r_{23}	0.2394	1.3241	0.6182	0.7853	1.2143	0.6855
r_{24}	0.1334	***1.5817***	*0.3163*	0.6147	1.3846	*0.4355*
r_{25}	0.1334	***1.5817***	*0.3163*	0.6147	1.3846	*0.4355*
r_{26}	0.2621	1	1	1	1	1
r_{27}	0.2621	1	1	1	1	1
r28	0.3908	0.8014	1.2334	1.1315	0.8687	1.1927
r29	0.1287	*0.3970*	***1.7086***	1.3994	0.6014	***1.5851***
r30	0.1287	*0.3970*	***1.7086***	1.3994	0.6014	***1.5851***
r31	2.6569	***1.6327***	0.6470	0.5971	1.2227	*0.3739*
r32	2.5006	***1.6412***	0.6614	0.5925	1.2161	*0.3648*
r33	0.8570	1	1	1	1	1
r34	0.0250	1	1	1	1	1
r35	0.4379	1	1	1	1	1
r36	0.4379	1	1	1	1	1
r37	0.4379	1	1	1	1	1
r38	0	–	–	–	–	–
r39	0	–	–	–	–	–
r40	1.0000	1	1	1	1	1
r41	0.8820	1	1	1	1	1
r42	2.8720	1	1	0.5378	0.5378	0.5378
r43	−0.0392	***44.9566***	**−16.2883**	***1.7347***	***46.6888***	**−13.3801**
r44	0.1311	1	1	***11.1251***	***11.1251***	***11.1251***
r45	2.6549	1	1	1	1	1
r46	2.6549	1	1	1	1	1
r47	2.6549	1	1	1	1	1
r48	3.3262	***1.6006***	0.7922	*0.4945*	1.1471	*0.2951*

The fluxes are normalized with respect to flux values in case 9

Change +50 % and more (*italics*); change −50 % and more (*bold italics*), change in direction (*bold*)

(r_{13}). Afterwards, by subsequent transformations through such intermediates as F6P (by reverse reaction of fructose-bisphosphatase [E.C. 4.1.2.13]), glucose-6-phosphate (catalyzed by PPK), 6-PG, and 2–dehydro–3–deoxy-phosphogluconate, the carbon source enters the EMP pathway at G3P and pyruvate nodes. According to Sichwart et al. [40], the wild strain does not harbor FBPA, but, according to Pohlmann et al. [30], the anabolic EMP is present. Hence, it was reasonable to pay special attention to this node (r_{13}) of metabolic network. In addition, without anabolic direction of r_{13}, the metabolic network (Fig. 1) was not functional (the glycerol metabolism was not possible). To ensure the first working hypothesis (i.e., the significance of the activity of the EMP pathway to generate G3P), it was necessary to impose constraint that r_{15} dominates over r_{13}. Results for such metabolic situation are presented in Fig. 5. To implement the second working hypothesis (i.e., the ED pathway is more active than the EMP pathway), two separate paths were followed: the first one in which r_{13} (with anabolic function) dominates over r_{15}, and another one in which r_4 dominates over r_{15}. Both mentioned conditions that favor ED have yielded exactly the same results that are presented in Fig. 6 (no difference if NAD/NADH or FAD/$FADH_2$ were included in reaction of GLY-3-P DH, no difference if r_5 was present or not).

Results presented in Figs. 5 and 6 can be interpreted in terms of flux differences between the EMP and ED pathways. In both figures and according to Tables 1 and 2, cases 3, 4, 7, 8, 11, 12, 15, and 16, it is observeable that the ED pathway needs the opposite direction for some reactions. That is particularly true for the glycolytic enzymes GA-3P DH (r_{15}), phosphoglycerate kinase (PGK, E.C. 2.7.2.3; r_{16}), phosphoglyceromutase (PGM, E.C. 2.7.5.3; r_{17}), and enolase (EN, E.C. 4.2.1.11; r_{18}) as well as for ribulose-5-phsosphate epimerase (R5PE, E.C. 5.1.3.4; r_7), and transketolase (TK, E.C. 2.2.1.1; r_{10}) (irrespective of NAD/NADH or FAD/$FADH_2$ in GLY-3-P DH, and irrespective of whether the r_5 is present or not). Additionally, if NAD contributes to the GLY-3-P DH reaction, triosephosphate isomerase (TPI, E.C. 5.3.1.1; r_{14}) changes the direction. Also, r_{43} (NAD(P)/NAD(P)H transhydrogenase) switches to the opposite direction (Table 1, cases 2, 6) if the EMP pathway dominates over the ED metabolic route and if 6-PG DH is present. The predominant metabolic flux through the ED pathway resulted in an additional effect: the fluxes of glyoxylate shuttle are increased, no matter if NAD or FAD is included in GLY-3-P DH and irrelevant of whether the 6-PG DH is present or not.

Domination of EMP pathway (catabolizing of G3P) over ED caused other occurrences, too: as expected, reactions of EMP enzymes (r_{14}–r_{19}) must be significantly increased to reach experimental yields (no matter whether NAD/NADH or FAD/$FADH_2$ are contributors for GLY-3-P DH, and irrelevant of whether the r_5 is present or not; Table 1, cases 2 and 6, and Table 2, cases 10 and 14). In addition, it has to be stressed that under such conditions, a reaction catalyzed by R5PE (r_7) must be extremely increased (valid if r_5 is present in the metabolic network).

When biomass growth is limited by ammonia, experimental finding for PHB yield on glycerol was 0.37 [mol mol^{-1}]. Theoretical in silico calculated yields using applied network are in the range of 0.3–0.5 [mol mol^{-1}]. This corresponds to 0.4–0.66 [mol C (mol C)$^{-1}$] (depending on combinations of elementary modes). These results are lower than those reported by Grousseau et al. [12] calculated for growth on butyric acid. In our calculations of metabolic fluxes, among tested metabolic situations (cases 1–16), we did not find any significant connection between IDH flux, PHB synthesis, and growth, but a significant correlation between the type of GLY-3-P DH cofactor (FAD vs. NAD) and the transhydrogenase action was confirmed. The necessity for desired activity of this enzyme is also connected with the ratio of glycerol metabolized through the ED/EMP pathways.

Conclusions

1. Under supposed intracellular steady-state conditions, 2,722 (NAD/NADH) and 2,701 (FAD/$FADH_2$) elementary modes were detected (presuming that NAD/NADH or FAD/$FADH_2$ are part of GLY-3-P DH system, respectively) for the established metabolic network representing *C. necator* metabolism when growing on glucose and glycerol.
2. Without PHB degradation and with glycerol as the sole carbon source, 202 (NAD/NADH) and 179 (FAD/$FADH_2$) elementary modes were detected regarding whether the pair NAD/NADH or FAD/$FADH_2$ contributes to the reaction of GLY-3-P DH, respectively. Among them, 188 (from set of 202) and 165 (from set of 179) were related to synthesis of new non-PHB biomass, to PHB, and to synthesis both of them simultaneously.
3. Only 43 elementary modes from a set of 188 and 36 from a set of 165 EMs represent the case of simultaneous production of PHB and residual biomass in the exponential growth phase.
4. Applied yield and elementary modes analysis has shown that the established metabolic network provides multiple solutions of the equation system in which the yields for biomass and PHB are equal to those obtained experimentally, when simultaneous synthesis of PHB and new biomass takes place. Experimentally calculated yields for biomass and PHB on glycerol can be in silico achieved when the ED dominates over EMP

route as well as if the EMP dominates over the ED route. In addition, the space of possible solutions was further expanded if NAD/NADH or FAD/$FADH_2$ were assumed to contribute to the reaction of GLY-3-P DH, as well as if 6-PG DH is present or not. Reliable data are available in the literature for the ancestor strain of *C. necator* DSM 545, namely *R. eutropha* H16. Different authors clearly state the predominate role of the ED pathway in the case of fructose and gluconate acting as a carbon source [8, 20]. Assumptions for the glycerol case regarding this and related strains are not reported in the present literature.

5. In order to clarify which of the mentioned metabolic situations de facto takes place in the real cellular system of *C. necator* DSM 545 cultivated on glycerol, the estimation of metabolic fluxes related to characteristic nodes in the network could be a helpful and indicative tool: node DHAP (r_{13}, r_{14}, r_{46}), node G3P (r_4, r_{10}, r_{13}, r_{14}, r_{15},r_{40}), measuring the difference in fluxes of glyceralde-3-P dehydrogenase and anabolic activity of FBPA, node G-6-P (r_1, r_2, r_{11},r_{40}) and node PYR (r_4, r_{19}, r_{20}, r_{31},r_{40}). This especially includes the activities of the enzymes TPI, FBPA (i.e., anabolic EMP direction), (PGA), and GA-3P DH.
6. Special attention should be paid to reactions catalyzed by R5PE (r_7), TK (r_{10}), PGK(r_{16}), PGM (r_{17}), EN (r_{18}), NAD(P)/NADH transhydrogenase (r_{43}): under some of the mentioned metabolic situations, these reactions change in silico their direction, or for some of them, the flux is significantly changed (glyoxylate shuttle enzymes). This reverse direction or activity level constitutes a strong indicator of preferred metabolic situation!
7. Based on in silico results, it cannot be concluded whether GLY-3-P DH uses NAD or FAD to accomplish its reaction, as well as it cannot be asserted whether *C. necator* DSM 545 possess 6-PG DH or not. Significant connection of the cofactor type of GLY-3-P DH (FAD or NAD) and transhydrogenase activity was indicated. The necessity for activity of this enzyme, connected with glycerol metabolizing pathways (ED or EMP), is also indicated.
8. Growth of *C. necator* DSM 545 on glycerol occurs very slowly [14, 48] but the same strain has given respectable results (without a long lag phase) when cultivated on glucose [21]. This strongly indicates that this strain possesses the metabolic capacity necessary for some reactions of PHB synthesis (concerning reactions in ED, downstream part of EMP, and Krebs cycle pathways). According to the applied model, similar results (as experimentally with glucose) can be achieved in silico with glycerol, but without limitations in the subsequent steps: glycerol transport, glycerol phosphorylation, GLY-3-P dehydrogenation, and the activity of anabolic part of EMP pathway. Based on the above, efforts in metabolic engineering should be concentrated on enhancing the glycerol transport system (r_{47}), on the constitutivity of glycerol-kinase (r_{46}) and glycerol-3-P dehydrogenase (r_{45}), as well as on minimizing the inhibitory effect of EMP substrates on the just-mentioned enzymes. Additional benefit could be achieved by improving the expression level of enzymes responsible for the anabolic EMP pathway in order to provide more C-flux through the ED pathway (aldolase, diphosphatase, isomerase, i.e., r_{11}–r_{13}/inclusive r_5 6-PG DH/Fig. 1), as well as by the enhanced expression of "downstream" EMP enzymes r_{15}–r_{19} in order to provide more biomass precursors and pyruvate (as precursor for AcCoA).

Acknowledgments This work was financially supported by the Collaborative EU-FP7 project ANIMPOL ("Biotechnological conversion of carbon containing wastes for eco-efficient production of high added value products"; Grant agreement No.: 245084). We are thankful to Dr. Matthias Raberg and Prof. Alexander Steinbüchel (UNI Münster), Dr. Anja Pöhlein and Prof. Rolf Daniel (UNI Göttingen) for useful information provided.

Conflict of interest All authors have agreed to submit the manuscript to the Journal of Industrial Microbiology and Biotechnology. The authors declare no conflict of interest.

References

1. Braunegg G, Sonnleitner B, Lafferty RM (1978) A rapid gas chromatographic method for the determination of poly-(b-hydroxy-butyric) acid in microbial biomass. Eur J Appl Microbiol Biotechnol 6:29–37
2. Burgard AP, Nikolaev EV, Schilling CH, Maranas CD (2004) Flux coupling analysis of genome-scale metabolic network reconstructions. Genome Res 14:301–312
3. Bushell ME, Sequeira SIP, Khannapho C, Zhao H, Chater KF, Butler MJ, Kierzek AM, Avignone-Rossa CA (2006) The use of genome scale metabolic flux variability analysis for process feed formulation based on an investigation of the effects of the *zwf* mutation on antibiotic production in *Streptomyces coelicolor*. Enzyme Microb Technol 39:1347–1353
4. Cavalheiro JMBT, Raposo RS, de Almeida MCMD, Cesário MT, Sevrin C, Grandfils C, da Fonseca MMR (2012) Effect of cultivation parameters on the production of poly(3-hydroxybutyrate-co-4-hydroxybutyrate) and poly(3-hydroxybutyrate-4-hydroxybutyrate-3-hydroxyvalerate) by *Cupriavidus necator* using waste glycerol. Bioresour Technol 111:391–397
5. Chen GQ (2009) A microbial polyhydroxyalkanoates (PHA) based bio- and materials industry. Chem Soc Rev 38:2434–2446
6. Dräger A, Kronfeld M, Ziller MJ, Supper J, Planatscher H, Magnus JB, Oldiges M, Kohlbacher O, Zell A (2009) Modeling metabolic networks in *C. glutamicum*: a comparison of rate laws in combination with various parameter optimization strategies. BMC Syst Biol 3:5. doi:10.1186/1752-0509-3-5
7. Edwards JS, Ramakrishna R, Schilling CH, Palsson BO (1999) Metabolic flux balance analysis. In: Lee SY, Papoutsakis ET (eds) Metabolic engineering. Marcel Dekker, New York, pp 13–57

8. Fleige C, Kroll J, Steinbüchel A (2011) Establishment of an alternative phosphoketolase-dependent pathway for fructose catabolism in *Ralstonia eutropha* H16. Appl Microbiol Biotechnol 91:769–776
9. Franz A, Song HS, Ramkrishna D, Kienle A (2011) Experimental and theoretical analysis of poly(β-hydroxybutyrate) formation and consumption in *Ralstonia eutropha*. Biochem Eng J 55:49–58
10. García IL, López JA, Dorado MP, Kopsahelis N, Alexandri M, Papanikolaou S, Villar MA, Koutinas AA (2013) Evaluation of by-products from the biodiesel industry as fermentation feedstock for poly(3-hydroxybutyrate-*co*-3-hydroxyvalerate) production by *Cupriavidus necator*. Bioresour Technol 130:16–22
11. Gombert AK, Nielsen J (2000) Mathematical modelling of metabolism. Curr Opi Biotechnol 11:180–186
12. Grousseau E, Blanchet E, Déléris S, Albuquerque MG, Paul E, Uribelarrea JL (2013) Impact of sustaining a controlled residual growth on polyhydroxybutyrate yield and production kinetics in *Cupriavidus necator*. Bioresour Technol 148:30–38
13. Gudmundsson S, Thiele I (2010) Computationally efficient flux variability analysis. BMC Bioinform 11:489. doi:10.1186/1471-2105-11-489
14. Kaddor C, Steinbüchel A (2011) Implications of various phosphoenolpyruvate-carbohydrate phosphotransferase system mutations on glycerol utilization and poly(3-hydroxybutyrate) accumulation in *Ralstonia eutropha* H16, AMB Express. 1:16. Available via http://www.amb-express.com/content/1/1/16
15. Khanna S, Goyal A, Moholkar VS (2012) Microbial conversion of glycerol: present status and future prospects. Crit Rev Biotechnol 32:235–262
16. Koller M, Bona R, Braunegg G, Hermann C, Horvat P, Kroutil M, Martinz J, Neto J, Pereira L, Varila P (2005) Production of polyhydroxyalkanoates from agricultural waste and surplus materials. Biomacromolecules 6:561–565
17. Koller M, Salerno A, Braunegg G (2013) Polyhydroxyalkanoates: basics, production and applications of microbial biopolyesters. In: Kabasci S, Stevens C (eds) Bio-based plastics: materials and applications. Wiley, New York, pp 137–170
18. König C, Sammler I, Wilde E, Schlegel HG (1969) Konstitutive Glucose-6-phosphat-Dehydrogenase bei Glucose verwertenden Mutanten von einem kryptischen Wildstamm. Arch Mikrobiol 67:51–57
19. Larhlimi A, Bockmayr A (2009) A new constraint-based description of the steady-state flux cone of metabolic networks. Discrete Appl Math 157:2257–2266
20. Lee JN, Shin HD, Lee YH (2003) Metabolic engineering of pentose phosphate pathway in *Ralstonia eutropha* for enhanced biosynthesis of poly-β-hydroxybutyrate. Biotechnol Prog 19:1444–1449
21. Lopar M, Vrana Špoljarić I, Atlić A, Koller M, Braunegg G, Horvat P (2013) Five-step continuous production of PHB analyzed by elementary flux modes, yield space analysis and high structured metabolic model. Biochem Eng J 79:57–70
22. Mahadevan R, Schilling CH (2003) The effects of alternate optimal solutions in constraint-based genome-scale metabolic models. Metab Eng 5:264–276 PMID 14642354
23. Orth JD, Thiele I, Palsson BØ (2010) What is flux balance analysis? Nat Biotechnol 28:245–248. doi:10.1038/nbt.1614
24. Papin JA, Price ND, Palsson BØ (2002) Extreme pathway lengths and reaction participation in genome-scale metabolic networks. Genome Res 12:1889–1900
25. Papin JA, Stelling J, Price ND, Klamt S, Schuster S, Palsson BO (2004) Comparison of network-based pathway analysis methods. Trends Biotechnol 22:400–405
26. Park JM, Kim TY, Lee SY (2010) Prediction of metabolic fluxes by incorporating genomic context and flux-converging pattern analyses. Proc Natl Acad Sci USA 107:14931–14936
27. Park JM, Kim TY, Lee SY (2011) Genome-scale reconstruction and *in silico* analysis of the *Ralstonia eutropha* H16 for polyhydroxyalkanoate synthesis, lithoautotrophic growth, and 2-methyl citric acid production. BMC Syst Biol 5:101. doi:10.1186/1752-0509-5-101
28. Pfeiffer T, Sánchez-Valdenebro I, Nuño JC, Montero F, Schuster S (1999) METATOOL: for studying metabolic networks. Bioinformatics 15:251–257
29. Pöhlein A, Kusian B, Friedrich B, Daniel R, Bowien B (2011) Complete genome sequence of the type strain *Cupriavidus necator* N-1. J Bacteriol 193:5017
30. Pohlmann A, Fricke WF, Reinecke F, Kusian B, Liesegang H, Cramm R, Eitinger T, Ewering C, Pötter M, Schwartz E, Strittmatter A, Voss I, Gottschalk G, Steinbüchel A, Friedrich B, Bowien B (2006) Genome sequence of the bioplastic-producing "Knallgas" bacterium *Ralstonia eutropha* H16. Nat Biotechnol 24:1257–1262
31. Price ND, Reed JL, Papin JA, Wiback SJ, Palsson BO (2003) Network-based analysis of metabolic regulation in the human red blood cell. J Theor Biol 225:185–194
32. Raberg M, Kaddor C, Kusian B, Stahlhut G, Budinova R, Kolev N, Bowien B, Steinbüchel A (2012) Impact of each individual component of the mutated PTS(Nag) on glucose uptake and phosphorylation in *Ralstonia eutropha* $G^{+}1$. Appl Microbiol Biotechnol 95:735–744
33. Raberg M, Peplinski K, Heiss S, Ehrenreich A, Voigt B, Döring C, Bömeke M, Hecker M, Steinbüchel A (2011) Proteomic and transcriptomic elucidation of the mutant *Ralstonia eutropha* G+1 with regard to glucose utilization. Appl Environ Microbiol 77:2058–2070
34. Reinecke F, Steinbüchel A (2009) *Ralstonia eutropha* strain H16 as model organism for PHA metabolism and for biotechnological production of technically interesting biopolymers. J Mol Microbiol Biotechnol 16:91–108
35. Schlegel HG, Gottschalk G (1965) Verwertung von Glucose durch eine Mutante von *Hydrogenomonas* H16. Biochem Z 341:249–259
36. Schuster S, Fell DA, Dandekar T (2000) A general definition of metabolic pathways useful for systematic organization and analysis of complex metabolic networks. Nat Biotechnol 18:326–332
37. Schuster S, Hilgetag C (1994) On elementary flux modes in biochemical reaction systems at steady state. J Biol Syst 2:165–182. doi:10.1142/S0218339094000131
38. Schwartz JM, Kanehisa M (2005) A quadratic programming approach for decomposing steady-state metabolic flux distributions onto elementary modes. Bioinformatics 21:204–205
39. Schweizer HP, Jump R, Po C (1997) Structure and gene-polypeptide relationships of the region encoding glycerol diffusion facilitator (glpF) and glycerol kinase (glpK) of *Pseudomonas aeruginosa*. Microbiology 143:1287–1297
40. Sichwart S, Hetzler S, Bröker D, Steinbüchel A (2011) Extension of the substrate utilization range of *Ralstonia eutropha* strain H16 by metabolic engineering to include mannose and glucose. Appl Environ Microbiol 77:1325–1334
41. Song HS, Morgan JA, Ramkrishna D (2009) Systematic development of hybrid cybernetic models: application to recombinant yeast co-consuming glucose and xylose. Biotechnol Bioeng 103:984–1002
42. Song HS, Ramkrishna D (2009) Reduction of a set of elementary modes using yield analysis. Biotechnol Bioeng 102:554–568
43. Steinbüchel A (1986) Expression of the *Escherichia coli pfkA* gene in *Alcaligenes eutrophus* and in other gram-negative bacteria. J Bacteriol 166:319–327
44. Stelling J, Klamt S, Bettenbrock K, Schuster S, Gilles ED (2002) Metabolic network structure determines key aspects of functionality and regulation. Nature 420:190–193

45. Stephanopoulos GN, Aristidou A, Nielsen J (1998) Metabolic engineering: principles and methodologies. Academic Press, San Diego
46. Varma A, Palsson BØ (1994) Metabolic flux balancing: basic concepts, scientific and practical use. Nat Biotechnol 12:994–998
47. von Kamp A, Schuster S (2006) Metatool 5.0: fast and flexible elementary modes analysis. Bioinformatics 22:1930–1931
48. Vrana Špoljarić I, Lopar M, Koller M, Muhr A, Salerno A, Reiterer A, Horvat P (2013) *In silico* optimization and low structured kinetic model of poly[(*R*)-3-hydroxybutyrate] synthesis by *Cupriavidus necator* DSM 545 by fed-batch cultivation on glycerol. J Biotechnol 168:625–635
49. Vrana Špoljarić I, Lopar M, Koller M, Muhr A, Salerno A, Reiterer A, Malli K, Angerer H, Strohmeier K, Schober S, Mittelbach M, Horvat P (2013) Mathematical modeling of poly[(*R*)-3-hydroxyalkanoate] synthesis by *Cupriavidus necator* DSM 545 on substrates stemming from biodiesel production. Bioresour Technol 133:482–494
50. Wang ZX, Bramer C, Steinbuchel A (2003) Two phenotypically compensating isocitrate dehydrogenases in *Ralstonia eutropha*. FEMS Microbiol Lett 227:9–16
51. Yu J, Si Y (2004) Metabolic carbon fluxes and biosynthesis of polyhydroxyalkanoates in *Ralstonia eutropha* on short chain fatty acids. Biotechnol Prog 20:1015–1024